第52回自動制御連合講演会
2009年11月21,22日(大阪大学)

素子バラツキを含んだ階層型ニューラルネットワークにおける確率共鳴現象

Stochastic resonance in a multi-layer neural network with population heterogeneity

○ 宇田川玲　浅井哲也　雨宮好仁
北海道大学大学院情報科学研究科
A. Utagawa, T. Asai, and Y. Amemiya
Graduate School of Information Science and Technology, Hokkaido University

Abstract　素子バラツキを含んだ階層型ニューラルネットワークにおける新しいタイプの確率共鳴現象について報告する。このニューラルネットワークは、ランダムな固定バラツキを持つ入力層、ダイナミック雑音を受ける中間層、および出力層の三層からなり、古典的なしきい系の確率共鳴モデルを空間的に重ね合わせたものに相当する（中間層のニューロンを近接する確率共鳴構造が共有する）。この重ね合わせの度合いを「ニューロンの受容野の大きさ」と考える。このネットワークに微弱な入力信号（中間層ニューロンのしきい値以下の入力）を与えた場合、入出力間の相関値が、中間層に加わる雑音の大きさ（>0）のみならず、受容野の大きさ（>0）に対しても最適値を持つことがわかった。

1 Introduction

Stochastic resonance (SR) has recently been spotlighted in the field of engineering, which is motivated by a wide variety of sensing applications to detect weak signals [1]. Recent challenges in electrical engineering revealed that SR could be observed in a laser [2, 3, 4], nonlinear electrical circuits [5, 6, 7], sigma-delta modulators [8], quantum circuits [9, 10, 11], and so on. Noise and fluctuations are usually considered as "obstacles" in electrical systems, and most strategies to deal with them are focused on the suppression. In contrast, SR in electrical systems certainly exploited noises to improve the SNR, which implies that a new kind of electrical systems would be evolved by utilizing noise and fluctuations (*e.g.*, [12, 13, 14]).

Recently, Funke *et al.* reported that a visual pathway in a cat primary visual cortex optimally utilized an SR-like process to improve signal detection while preventing spurious noise-induced activity and keeping the SNR high [15]. Although the mechanism is still unclear, one may assume that i) SR without optimal tuning of noise intensities [16] underlies the fundamental mechanism and ii) the visual pathway from photoreceptors to cortical neurons may cause extremely large receptive fields (RFs). Inspired by these results and assumptions, we here propose a simple neural network model that consists of an array of SR units where threshold elements are represented by McCulloch-Pitts (MP) neurons and the MP neurons are shared by the neighboring SR units, *i.e.*, the number of MP neurons in each SR unit represents the RF size. Our primary interest here is to investigate the model's fundamental behaviors as a function of the noise intensity, the RF size, and population heterogeneity (random offsets between the inputs) that was not discussed in [15].

2 Brief Review of SR Models

Figure 1 shows a basic SR model proposed in [16]. A subthreshold input is commonly given to N threshold elements, as illustrated in Fig. 1(a). FitzHugh-Nagumo neurons were used in the original paper, but one may use McCulloch-Pitts (MP) type neurons instead without loss of generality. Each neuron accepts external uncorrelated noises, which lead the neurons to fire with high (or low) possibility when the subthreshold input is high (or low). When the outputs were summed, the uncorrelated noises tend to be cancelled each other as N increases. Examples with MP type neurons were shown in Fig. 1(b) where correlation values between the input and output signals were plotted as a function of the noise intensity. One can observe that the correlation values are increased as N increases and the values tend to be insensitive to noise intensity (> 0.2 when $N = 100$). This means, when a large number of neurons are used in the system, the subthreshold (weak) input can be detected without optimal tuning of the noise intensity [16].

The concept of SR has been expanded to image sensing applications [17]. Let us consider a 2-D array of pixels, and assume that each pixel consists of the same SR model in Fig. 1(a). The array accepts dark (subthreshold) images, and thus the array's output would be always zero when external noises were not given. As the noise intensity increases, nonzero outputs appeared, as shown in Figs. 2(a) to (c). When each pixel has random offset values, they are directly detected through the SR process, as shown in Figs. 2(d) to (f). Consequently, SR would be useful for sensing weak signals (*e.g.*, dark images), however, the random offsets would also be detected in practical systems. Note that such a random offset is generally observed in photodiodes as dark currents, and the dark currents are cancelled by correlated double sampling (CDS) circuits in many CMOS image sensors [18]. Here we do not argue that SR may defeat CDS, but are interested in SR-based image pro-

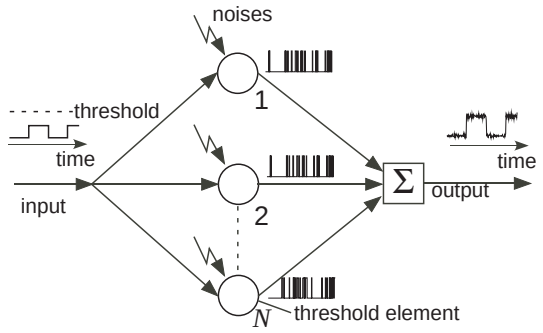

(a) Summing network of threshold elements

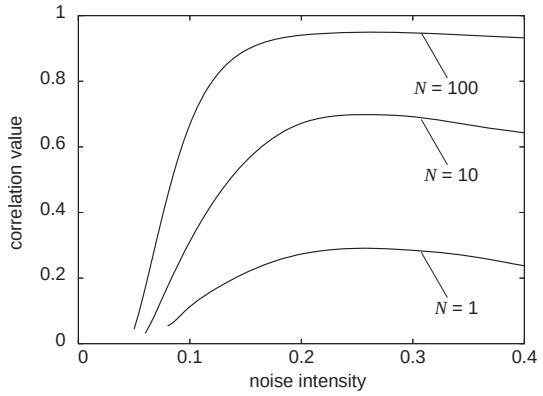

(b) Correlation values between input and output signals vs noise intensity

Figure 1: Stochastic resonance (SR) without optimal tuning of noise intensity [16]

cessing that may exist in biological vision systems.

3 Neural Networks with Locally-Coupled SR Units

We here propose a simple neural network model for SR-based image processing. Our model accepts images (optical inputs), and generates the outputs through an SR process, as demonstrated in Fig. 2. Three types of array structures of SR units are considered, as shown in Fig. 3. The first structure is illustrated in Fig. 3(a) where an optical input to a pixel is given to a single noisy MP neuron. Each neuron accepts temporal noises, and the temporal average of the neuron's output represents the pixel output. With this setup, the maximum correlation values between the input and the output would be low because the single pixel exactly corresponds to the network of $N = 1$ in Fig. 1. To increase the correlation value, one can employ the second structure where multiple MP neurons are embedded in each pixel ($N = 3$ for example), as shown in Fig. 3(b). This setup certainly increases the correlation values, and the model would exhibit the best (but trivial) results with large N. Our interest here is to introduce receptive fields (RFs) in an array of SR units where MP neurons are shared by the neighboring SR units, as shown in Fig. 3(c). It should be noticed that

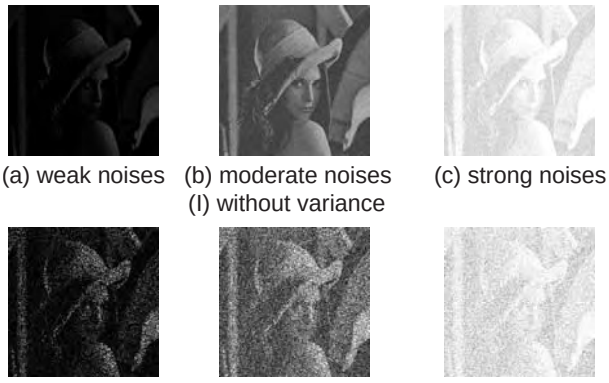

(a) weak noises (b) moderate noises (c) strong noises
(I) without variance

(d) weak noises (e) moderate noises (f) strong noises
(II) with variance

Figure 2: 2-D examples of weak-signal (dark-image) sensing with SR.

an SR unit with $N = 3$ is hidden in this structure (illustrated by solid lines and circles in Fig. 3(c) left), and the MP neurons are shared by the neighboring SR units.

In Fig. 3(c), the optical input distribution is represented by $I(x)$, and is accepted by nominal photoreceptors. The output distribution of the photoreceptors is defined by $I(x)+\delta(x)$ where $\delta(x)$ represents the spatial random noise (pixel variations) given by $m \cdot N(0,1)$ [$N(0,1)$ is the Gaussian noise with zero mean and unity standard deviation]. Inputs to MP neurons via local coupling connections between photoreceptors and MP neurons were then defined by

$$R(x) = \int \big(I(X) + \delta(X)\big) \cdot g(X - x)\, dX, \qquad (1)$$

$$g(x) = \frac{1}{\sqrt{2\pi}\sigma} \exp\left[-\frac{x^2}{2\sigma^2}\right],$$

where σ represents the RF size. The output distribution of the MP neurons is thus

$$V(x) = H\big(R(x) - \xi(t)\big), \qquad (2)$$

where $H(\cdot)$ represents a step function, and $\xi(t)$ the temporal random noise given by $A \cdot N(0,1) + \theta$ (A: standard deviation, θ: mean threshold). The final output via local coupling connections between the MP neurons and the output cells is given by

$$O(x) = \int V(X) \cdot g(X - x)\, dX. \qquad (3)$$

With this model, we examine SR behaviors by changing m (spatial randomness), σ (RF size), and A (temporal randomness being necessary for SR).

4 Results

We conducted numerical simulations to investigate effects of RF sizes and noises (random offsets in photoreceptors and temporal noises in MP neurons). In the following

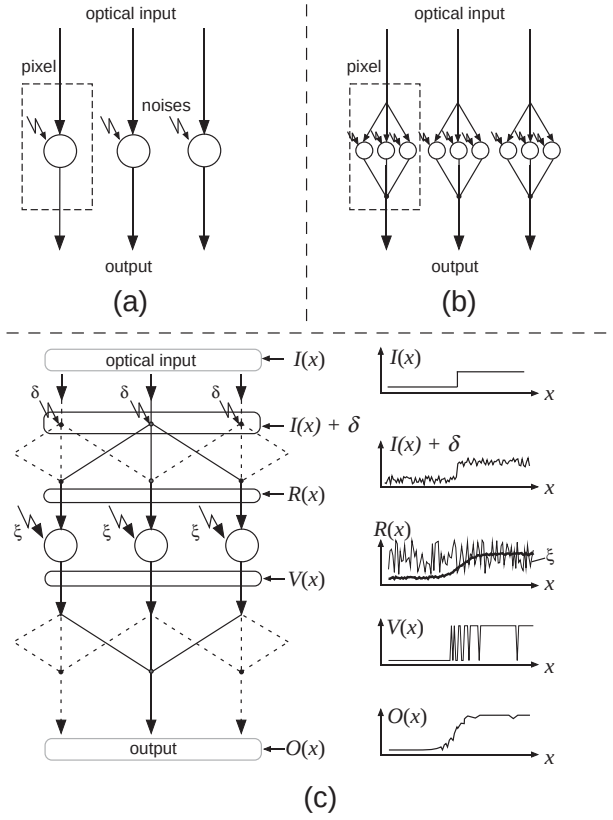

Figure 3: Three types of SR models. (a) SR array with $N = 1$, (b) $N = 3$ and (c) proposed SR array having local connections where one pixel with $N = 3$ shown in (b) is hidden (solid lines and circles).

simulations, we assume $\theta = 0.5$ and $I(x) = 0.3 \cdot H(x - 0.5)$. The 1-D space ($x : [0, 1]$) is discretized with 32 MP neurons ($N = 32$) where $dx \equiv 1/N$ and $x = i \cdot dx$ (i: integer value). Figure 4 (top) shows density plots of correlation values between the optical input $I(x)$ and final output $O(x)$ as a function of σ and A with four different values of ms. The output $O(x)$ was obtained by averaging results of 512 trials with different random seeds. The correlation values were calculated by

$$C \equiv \frac{\sum_{i=1}^{N}[I(i \cdot dx) - \langle I\rangle] \cdot [O(i \cdot dx) - \langle O\rangle]}{\sqrt{\sum_{i=1}^{N}[I(i \cdot dx) - \langle I\rangle]^2}\sqrt{\sum_{i=1}^{N}[O(i \cdot dx) - \langle O\rangle]^2}}, \quad (4)$$

where $\langle I\rangle$ and $\langle O\rangle$ represent the spatially averaged distributions of $I(x)$ and $O(x)$ ($\langle I\rangle$ is 0.15, and $\langle O\rangle$ was numerically calculated from $O(x)$). Figure 4 (bottom) shows distributions of $I(x)$, $O(x)$, and random threshold $\xi(t)$ at arbitrary t. If photoreceptors are identical ($m = 0$, Fig. 4(a)), the maximum correlation value was obtained when the RF size (σ) was zero, as expected. However, if photoreceptors are not identical ($m = 0.1$, Fig. 4(b)), the correlation peak was moved to nonzero σ while keeping the peak value high. This implies that a nonzero RF size would be necessary for SR among nonidentical components. As m increases (Fig. 4(c) and (d)), the peak shifted to higher σ, however, the peak values were decayed slowly.

Figure 5 shows horizontal cross sections of Fig. 4(b). As in the basic SR network (Fig. 1), the correlation values had a peak for variable noise intensity (A). It should be noticed that the correlation values did not decrease suddenly as noise intensity A increased. When $\sigma = 1.5$, for example, the peak value was almost insensitive within $0.2 < A < 0.5$. Since σ qualitatively represents the number of neurons in the RF of each pixel, increasing σ may improve the correlation as in the basic SR network. However, nonzero σ causes smoothing of the optical input. Therefore there may exist upper bounds of σ. Figure 6 shows the vertical cross sections of Fig. 4(b) representing correlation values as a function of σ. The peak value was obtained around $\sigma \approx 1.5$ and $A = 0.4$, which proves that nonzero σ (RF size) is necessary for obtaining higher correlation values in this SR system with nonidentical pixels ($m > 0$).

To confirm the effects of convergent coupling connections between $V(x)$ and $O(x)$ in our SR model, we calculated peak correlation values between $I(x)$ and $O(x)$ (C_{IO}) as well as correlation values between $I(x)$ and $V(x)$ (C_{IV}). Figure 7 plots the peak values as a function of spatial variance m ($I(x) = 0.1 \cdot H(x - 0.5)$). For given m, the peak values were scanned by sweeping two parameters A (noise intensity) and σ (RF size). We observed an apparent difference between C_{IO} and C_{IV}, where C_{IO} was always larger than C_{IV}, and the difference expanded significantly as m increased. This result proves that employing the coupling connections between $V(x)$ and $O(x)$ is effective for increasing the correlation values, which results in improving quality of detected images.

Finally, we evaluated performances of a 2-D network with two distinct RF sizes ($\sigma = 0.3,\ 1.5$). Figure 8 shows the results ($A = 0.4$, $m = 0.1$, and $\theta = 0.5$). The binary input image $I(x, y)$ is shown in Fig. 8(a) [32×32-pixels black and white image. $I(x, y)$ = 0 (black) and 0.3 (white)], whereas level-adjusted density plots of outputs of neurons $V(x, y)$ [(b) and (c)] and final output cells $O(x, y)$ [(d) and (e)] with different RF sizes are shown. By comparing the final outputs of small RF ($\sigma = 0.3$) and relatively large RF ($\sigma = 1.5$), we first conclude that expanding RF sizes is useful for obtaining visually-better output image through SR among nonidentical pixels, if the input image is not complex (realistic). The important thing here is that the underlying mechanism of the performance increase mainly resulted from convergence on $O(x, y)$ with nonzero σ (=1.5), as proved in Fig. 7.

Figure 9 shows simulation results for realistic gray-scale input images. Figure 9(a) represents the input image [256 × 256-pixels 8-bit gray-scale image. $I(x, y)$s were renormalized to 0 (black-most pixel) and 0.3 (white-most pixel)]. When $\sigma = 0.3$, the output image detected by SR was very noisy (Fig. 9(b)), which represents a raw image including random offsets detected by SR. Figures 9(c) and (d) show level-adjusted distributions of $V(x, y)$ and $O(x, y)$, respectively, when $\sigma = 1.5$. The difference in image qualities

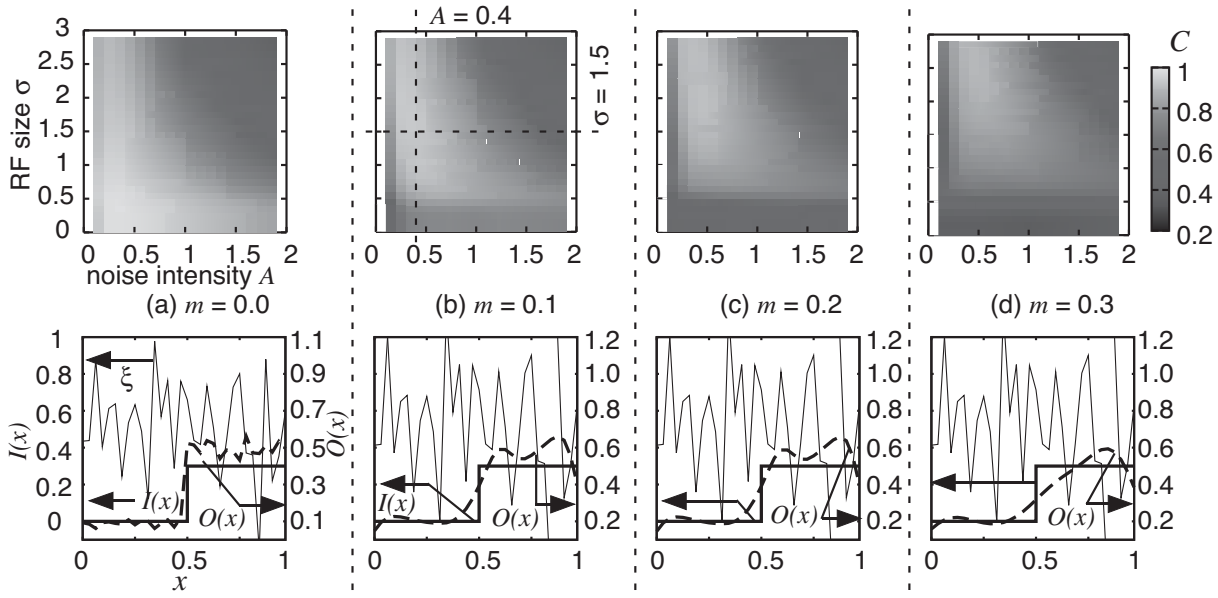

Figure 4: Simulation results of proposed 1-D network for step optical inputs

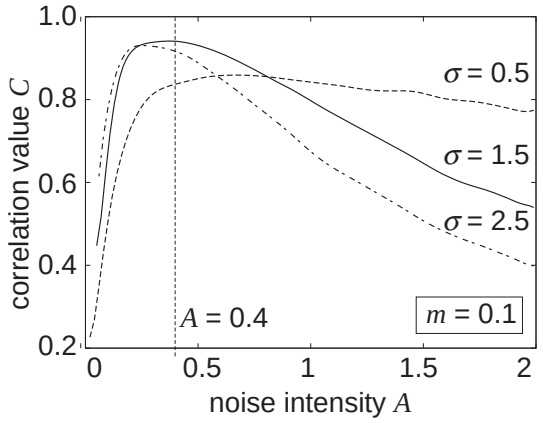

Figure 5: Horizontal cross sections of Fig. 4(b).

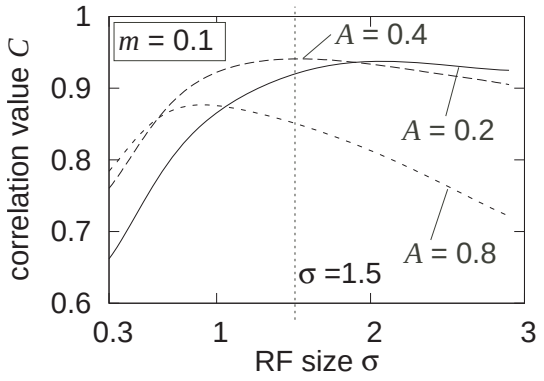

Figure 6: Vertical cross sections of Fig. 4(b).

between Figs. 9(c) and (d) were not apparent at-a-glance view, however, there is quantitative difference certainly, as shown in Fig. 7.

We have shown that the maximum correlation value between input $I(x)$ and output $O(x)$ was obtained by setting optimal noise intensity A and receptive field (RF) size σ (Fig. 6). Figure 5 showed well-known SR characteristics, where subthreshold inputs $I(x)$ given to MP neurons were nominally amplified by applying temporal noises to the neurons. Moreover, a new type of SR was observed in Fig. 6 where maximum correlation value was obtained at certain value of RF size σ.

Here let us consider the reason why correlation value is maximized by non-zero σ. MP neurons receiving temporal noises may respond to subthreshold inputs if the sum of the inputs and the noise intensities exceed the threshold values. The response strongly depends on the noise sequences, *i.e.*, the neuron's output would be 1-bit temporal random sequences (time varying sequences of 0 and 1). When output $V(x)$ is averaged over time, the averaged value $\overline{V}$ converges to static values. If noises were applied to the neurons with optimal intensity, $\overline{V}$ converges to the subthreshold input, *i.e.*, $\overline{V}$ is strongly correlated with the input. Thus, the output of the MP neuron can be represented by its input.

Our model has two local-coupling layers, as shown in Fig. 3(c). One layer connects photoreceptors and MP neurons, and another connects the MP neurons and the output cell. Our results showed that these coupling connections (nonzero σ) were effective for decreasing spatial variance m in photoreceptors, which resulted in increase of correlation values between the noiseless input $I(x)$ and the model's output $O(x)$. The correlation value was nonmonotonically increased as the RF size (σ) increased (Fig. 6).

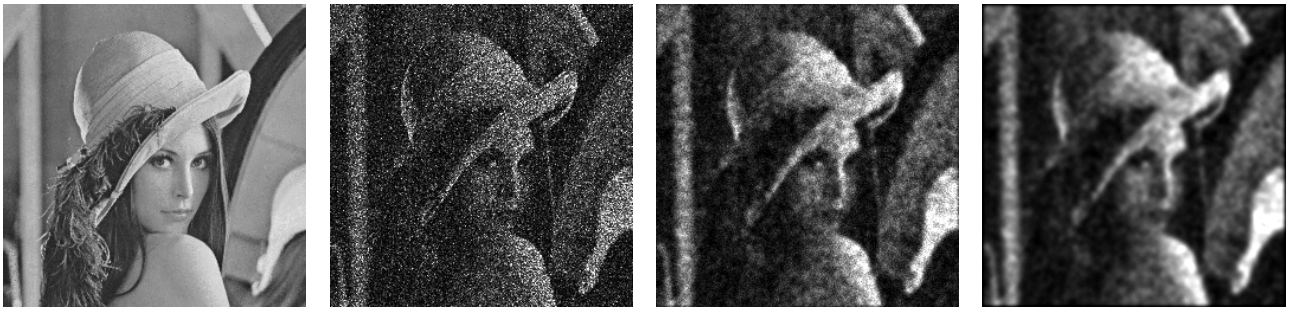

(a) input image $I(x, y)$ (256×256 8-bit gray-scale) | (b) output $O(x, y)$ with small RF ($\sigma = 0.3$) | (c) output $V(x, y)$ with large RF ($\sigma = 1.5$) | (d) output $O(x, y)$ with large RF ($\sigma = 1.5$)

Figure 9: 2-D simulation results using gray-scale images. Grayscale output images (b-d) were obtained by averaging binary results of 512 trials with different random seeds.

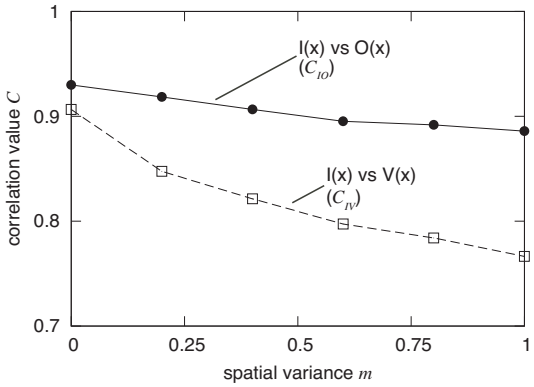

Figure 7: Maximum correlation values vs spatial variance

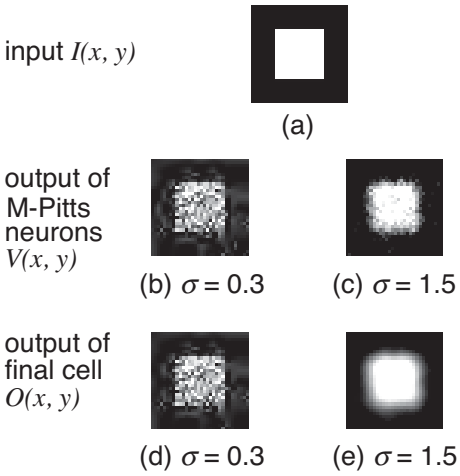

Figure 8: 2-D simulation results with test pattern image. Gray-scale output images (b-e) were obtained by averaging binary results of 512 trials with different random seeds.

When m is increased, the correlation values would be decreased due to the nonzero σ. It should be noted that if $m = 0$, the maximum correlation value is certainly 1, however, the maximum value would be decreased as m increased because of the mismatches between $I(x)+\delta$ and output $O(x)$.

The network shown in Fig. 3(c) with small σ are considered to have the same characteristic as the conventional SR network shown in Fig. 3(a). Therefore, time-averaged output $\overline{O}$ in Fig. 3(c) is equal to the input of the MP neurons ($\overline{V}$), as described above. Thus, when $m > 0$, $\overline{O}$ approaches to $I(x) + \delta(x)$. When m approaches to the signal level of $I(x)$, the correlation value between input $I(x)$ and output $O(x)$ ($\approx I(x)+\delta(x)$) would be low values. As σ increases, the correlation value is also increased because nonzero σ was effective for decreasing m, as described above. Further increase of σ results in the decrease of the correlation value. Remember that input distribution of MP neuron ($R(x)$) was defined by the convolution of $I(x) + \delta$ and coupling weight function $g(x)$ in Eq. (1). This means that, with extremely large σ, the spatial variance in $R(x)$ vanishes when a uniform $I(x)$ is given. On the other hand, the correlation value decreases due to the mismatches of $I(x)$ and extremely smoothed $O(x)$. Consequently, the spatial variance m is strongly suppressed by constructing the superimposed structure of SR units.

5 Conclusion

We proposed a simple neural network consisting of locally-coupled stochastic resonance (SR) units with nonidentical photoreceptors. Through numerical simulations, we observed a new class of SR among the units when the photoreceptors had random offsets. We calculated correlation values between the optical inputs and the output as a function of the receptive-field (RF) size and intensities of the random components in photoreceptors and the McCulloch-Pitts neurons. We then showed that there existed nonzero optimal sizes of the RF as well as optimal noise intensities of the neurons under the nonidentical photoreceptors. Furthermore, we demonstrated 2D SR with the proposed model, and showed that the difference in image qualities between a simple-smoothing model with SR and smoothing-

plus-convergent model with shared SR was not apparent at a glance, although there existed a quantitative difference between them.

References

[1] F. Moss, L.L. Ward, and W.G. Sannita, "Stochastic resonance and sensory information processing: a tutorial and review of application," *Clinical Neurophysiology*, vol. 115, pp. 267–281, 2004.

[2] V. Gautam and R. Rajarshi, "Stochastic resonance in a bistable ring laser," *Phys. Rev. A*, Vol. 39, no. 9, pp. 4668–4674, 1989.

[3] A. Fioretti, L. Guidoni, R. Mannella, and E. Arimondo, "Evidence of stochastic resonance in a laser with saturable absorber: Experiment and theory," *J. Statistical Phys.*, Vol. 70, No. 1–2, pp. 403–412, 2005.

[4] L. Zhang, "Stochastic resonance in a single-mode laser driven by quadratic pump noise and amplitude-modulated signal", *Chinese Phys. B*, Vol. 18, pp. 1389–1393, 2009.

[5] F. Moss, J.K. Douglass, L. Wilkens, D. Pierson, and E. Pantazelou, Stochastic Resonance in an Electronic FitzHugh-Nagumo Model, Stochastic processes in astrophysics, J.R Buchler and H.E. Kandrup Eds., Annals of the New York Academy of Sciences, Vol. 706, The New York Academy of Sciences, New York, p. 26, 1993.

[6] V.S. Anishchenko, I.A. Khovanov, and B.V. Shulgin, "Stochastic resonance in passive and active electronic circuits", *Chaotic, Fractal, and Nonlinear Signal Processing*, Vol. 375, pp. 363–381, 1996.

[7] O. Calvo and D.R. Chialvo, "Ghost stochastic resonance in an electronic circuit," *Int. J. Bifurcation and Chaos*, Vol. 16, No. 3, pp. 731–735, 2006.

[8] O. Oliaei, "Stochastic resonance in sigma-delta modulators," *Electronics Lett.*, Vol. 39, No. 2, pp. 173–174, 2003.

[9] T. Oya, T. Asai, and Y. Amemiya, "Stochastic resonance in an ensemble of single-electron neuromorphic devices and its application to competitive neural networks," *Chaos, Solitons and Fractals*, Vol. 32, No. 2, pp. 855–861, 2007.

[10] S. Kasai and T. Asai, "Stochastic resonance in Schottky wrap gate-controlled GaAs nanowire field effect transistors and their networks," *Applied Physics Express*, Vol. 1, 083001, 2008.

[11] S. Kasai, "Investigation on stochastic resonance in quantum dot and its summing network," *Int. J. Nanotechnology and Molecular Computation*, Vol. 1, No. 2, pp. 70–79, 2009.

[12] T. Oya, I.N. Motoike, and T. Asai, "Single-electron circuits performing dendritic pattern formation with nature-inspired cellular automata," *Int. J. Bifurcation and Chaos*, Vol. 17, No. 10, pp. 3651–3655, 2007.

[13] A. Utagawa, T. Asai, T. Hirose, and Y. Amemiya, "An inhibitory neural-network circuit exhibiting noise shaping with subthreshold MOS neuron circuits," *IEICE Trans. Fundamentals*, Vol. E90-A, No. 10, pp. 2108–2115, 2007.

[14] A. Utagawa, T. Asai, T. Hirose, and Y. Amemiya, "Noise-induced synchronization among sub-RF CMOS analog oscillators for skew-free clock distribution," *IEICE Trans. Fundamentals*, Vol. E91-A, No. 9, pp. 2475–2481, 2008.

[15] K. Funke, N.J. Kerscher, and F. Wörgötter, "Noise-improved signal detection in cat primary visual cortex via a well-balanced stochastic resonance like procedure," *European J. Neuroscience*, Vol. 26, No. 5, pp. 1322–1332, 2007.

[16] J.J. Collins, C.C. Chow, T.T. Imhoff, "Stochastic resonance without tuning," *Nature*, Vol. 376, pp. 236–238, 1995.

[17] E. Simonotto, M. Riani, C. Seife, M. Roberts, J. Twitty, and F. Moss, "Visual perception of stochastic resonance," *Phys. Rev. Lett.*, Vol. 78, No. 6, pp. 1186–1189, 1997.

[18] C.C. Enz and G.C. Temes, "Circuit techniques for reducing the effects of op-amp imperfections: autozeroing, correlated double sampling, and chopper stabilization," *Proceedings of the IEEE*, Vol. 84, No. 11, pp. 1584–1614, 1996.